Asian Journal of Chemistry; Vol. 29, No. 2 (2017), 287-290

ASIAN JOURNAL OF CHEMISTRY

http://dx.doi.org/10.14233/ajchem.2017.20163

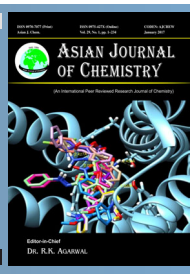

Photocatalytic Activity and Antimicrobial Properties of TiO_2-SiO_2-PVA Composite

SRI WAHYUNI[1,*], AGUNG TRI PRASETYA[1,*] and INDRIANA KARTINI[2]

[1]Department of Chemistry, Faculty of Mathematics and Natural Sciences, Universitas Negeri Semarang, Gunung Pati 50229, Indonesia
[2]Department of Chemistry, Faculty of Mathematics and Natural Sciences, Universitas Gadjah Mada, Sekip Utara, Yogyakarta, 55281, Indonesia

*Corresponding authors: E-mail: sri.wahyuni2808@mail.ugm.ac.id; zifaluqi@gmail.com

Received: 1 July 2016; *Accepted*: 28 September 2016; *Published online*: 30 November 2016; AJC-18146

A series of silica-titania nanocomposite with different mole ratios was prepared in the presence of polyvinyl alcohol by the sol-gel method. Several characterization techniques were adopted such as N_2-adsorption-desorption, X-ray diffraction, Fourier transform infrared spectroscopy, transmission electron microscope and scanning electron microscope connected with energy dispersive spectroscopy. The photocatalytic activity of the composites was investigated using methylene blue as a model pollutant. The results showed that the TiO_2-SiO_2 composites give a better performance than TiO_2 alone. The TiO_2-SiO_2-30 composites (SiO_2/TiO_2 mole ratio = 0.3) gives the best result of methylene blue removal among the synthesized composites. The antimicrobial activity of the composites was evaluated by observing the inhibition of *E. coli* growth under UV irradiation at a wavelength of 368 nm. All nanocomposites give antimicrobial activity by inhibiting *E. coli* growth except the composite without UV irradiation.

Keywords: Nanocomposite, Sol-gel method, Antimicrobial activity.

INTRODUCTION

In the last two decades, due to the non-toxic and its special properties, titanium oxide nanoparticles have attracted a great deal of attention as potential photocatalysts to address urgent and global environmental concerns. The photocatalytic degradation of various toxic compounds in aqueous solutions using fine titanium oxide particles has been studied by many researchers [1-3]. Titanium dioxide has been widely used as a white pigment in a broad variety of applications, such as coatings, cosmetics, food stuff and extensive potential applications, due to its unique physical and chemical properties. Titanium dioxide is largely used as photocatalyst due to its beneficial characteristics *e.g.*, high photocatalytic efficiency, physical and chemical stability, low cost and low toxicity [4-6]. It is well known that TiO_2 in anatase crystalline form, which is biologically and chemically inert, can be used as an excellent photocatalyst material in the hydrophilic self-cleaning coatings and widespread photocatalytic purposes under UV/visible light irradiation [7].

Recently, silica, titania and silica-titania materials have been obtained by sol-gel methods extensively. The sol-gel process is expected to offer unique advantages for the preparation of such highly dispersed materials photocatalysts, especially to be applied to coating material, active thin film photocatalysts and multicomponent ceramics [8-10]. The chemical and physical properties of titania-silica material depend on both the composition and the degree of homogeneity. Therefore, different synthesis strategies have been developed such as co-precipitation, flame hydrolysis, impregnation and chemical vapour deposition [11]. The sol-gel route has demonstrated a high potential for controlling the bulk and surface properties of the oxides [12,13]. In the present study, TiO_2-SiO_2 nanocomposite was synthesized *via* the sol-gel method in the presence of polyvinyl alcohol at room temperature [14]. TiO_2-SiO_2 composites are very promising in the field of heterogeneous photocatalysis since they could enhance photocatalytic activity compared to pure TiO_2 photocatalyst. The effect of mole ratio SiO_2/TiO_2 on particles size and photocatalytic activity were investigated.

EXPERIMENTAL

The chemicals used in this study were titanium tetraisopropoxide (TTIP, 97 %, Sigma), as a titanium precursor, tetraethylorthosilicate (TEOS, 98 %, E-Merck), as silica source, polyvinyl alcohol (PVA) (E-Merck); methylene blue, HCl, NH_3 (25 wt %) and anhydrous ethanol (C_2H_5OH) from Merck. *Escherichia coli* (FNCC0051), were from laboratory stock of the Biological Sciences Department of Semarang State University. Other materials for bacteria cultivation, such as agar, yeast extract, sodium chloride, tryptone and plastic and Pyrex Petri dishes were used from conventional laboratory stock.

General procedure: The TiO_2-SiO_2 (TS) composite was prepared by the following method. In the synthesis of Sol A, TTIP was used as a precursor and was mixed with ethanol, aqueous solution of 0.1 M HCl and deionized water in the volume ratio 1:2:2:2, respectively. The mixture was stirred for 1 h and maintained in the pH range from 1 to 2. In Sol B, TEOS was mixed with 40 mL ethanol under nitrogen atmosphere and stirred for 1 h. Sol A was then added into Sol B and the mixture was stirred for 3 h at 60 °C. The aqueous solution of PVA (1 %) was added to the above mixture at the rate of 0.5 mL/min and was stirred for 2 h. The gel was dried at room temperature. Finally, the mixture was heated at 120 °C for 1 h. The powder was calcined at 500 °C for 3 h. The composite produced was denoted as TiO_2-SiO_2.

Detection method: Phase identification of the products was carried out by X-ray diffraction (XRD) obtained on Shimadzu diffractometer using CuK_α line radiation. The crystallite size of the samples was determined by Scherrer equation [11]. Functional group analysis of the nanocomposite was performed using a Fourier transform infrared (FT-IR) spectrometer (Shimadzu-FTIR-8201PC). The morphology of the products was studied by transmission electron microscope (TEM, JEOL_JEM 1400). The specific surface area of the samples was determined by nitrogen adsorption-desorption using a surface area analyzer (NOVA Quantachrome). Surface morphology and their composition were studied using scanning electron microscope-energy dispersive spectroscopy (SEM-EDS) (Model JEOL JSM-6510LA).

Photocatalytic activity of the synthesized nanocomposites was evaluated by the degradation of methylene blue. All of the experiments were conducted in an opened Pyrex vessel of 50 mL capacity. The UV-B lamp was used as light source. The distance between the UV source and the vessels containing reaction mixture was fixed at 15 cm [15]. Antimicrobial activity of the nanocomposites was evaluated by agar dilution methods with *E. coli* as microbial tests [16]. The synthesized titanium dioxide agar plates were irradiated in a UV box, which contained four fluorescent blacklight tubes, 10 W each, with λ_{max} 368 nm [17]. The sample plates were collected immediately after the titanium dioxide agar plates were exposed to UV light for 60 min. The test plates were incubated at 36 °C for 18 h. The results then were inspected visually and the growth of the colony of bacteria was recorded. All tests and inoculation on each plate were run in duplicate [16].

RESULTS AND DISCUSSION

Fig. 1 shows the XRD patterns of TiO_2 and nanosized TiO_2-SiO_2 (with varying molar ratio of SiO_2/TiO_2) samples. All materials were calcined under the same condition in air at 500 °C for 3 h. TiO_2 and nanosized TiO_2-SiO_2 showed a clear anatase-type crystal structure. The sharp peaks and strong intensities indicated that crystallization was present and the higher the percentage of TiO_2 gave the higher intensity of peaks. The crystallite type of the TiO_2-SiO_2 nanocomposite particles was the pure anatase. The most intense reflection at $2\theta = 25.5°$ is assigned to anatase (d101). Not much difference has been detected between patterns of TiO_2 and TiO_2-SiO_2 composites. The powders showed the crystalline pattern and

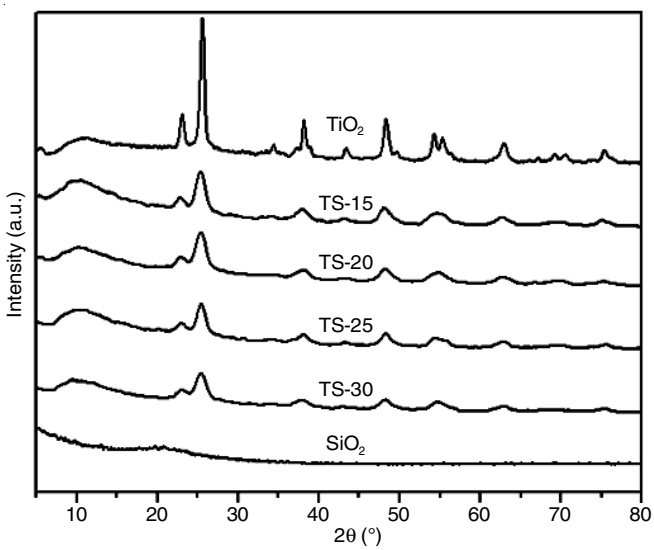

Fig. 1. XRD patterns of TiO_2 and TiO_2-SiO_2 at various molar ratios of SiO_2/TiO_2

the observed 'd' lines match the reported values for the anatase phase. The intensity of the characteristic peak of TiO_2 anatase phase decreased for TiO_2-SiO_2 compared to pristine TiO_2 due to the inclusion of amorphous SiO_2. The decrease in crystallinity of titania by silica addition indicates that the crystalline anatase phase can be incorporated in the amorphous silicate framework by the formation of a solid solution of anatase and silica [17]. The peak associated with SiO_2 show that it is an amorphous form of silica. From the wide diffraction peaks, it can be deduced that the TiO_2 and TiO_2-SiO_2 particles are nanosized [18]. The grain size determined from the XRD pattern using the Sherrer formula is around 11-19 nm. The crystallite sizes of TiO_2 and TiO_2-SiO_2 are listed in Table-1.

TABLE-1
CRYSTALLITE SIZE AND BET SURFACE AREA OF TiO_2 AND TiO_2-SiO_2

Catalysts	Phase	Crystallite size (nm)	Calcinations (°C)	Surface area (BET, m^2/g)
TiO_2	Anatase	19.57	450	98.0
TiO_2-SiO_2-15	Anatase	16.17	500	113.2
TiO_2-SiO_2-20	Anatase	15.53	500	184.4
TiO_2-SiO_2-25	Anatase	13.90	500	194.4
TiO_2-SiO_2-30	Anatase	11.90	500	214.8

The crystallite size data (Table-1) shows that the amount of SiO_2 sphere has an effect on the crystallite size of grafted nanosized TiO_2, with a higher amount of SiO_2 resulting in smaller crystallite size. This effect may be due to the SiO_2 limiting the agglomeration of TiO_2 particles. Studies showed that addition of silica or alumina also increases the anatase phase stability of titania [19]. SiO_2 enhancing the homogeneity of distribution of TiO2 in the surface of material. On the other hand, the colloidal TiO_2-SiO_2 nanocomposites exhibited regular morphology since the TiO_2-SiO_2 cores were coated by PVA. The average particle size of the colloidal TiO_2-SiO_2 nanocomposites was measured to be 11.90 to 16.17 nm.

Fig. 2 represents the FT-IR spectra of the sol–gel derived nano TiO_2-SiO_2-PVA composites. The peaks at 3402 cm^{-1} and 1628 cm^{-1} in the spectra are due to the stretching and bending

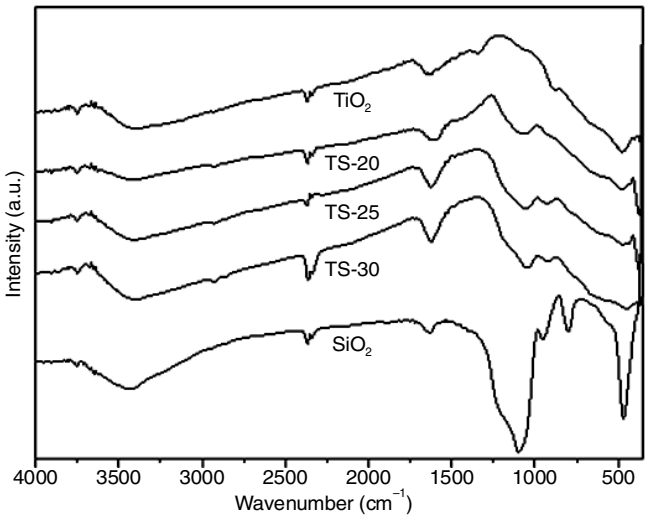

Fig. 2. FT-IR spectra for Titania-Silica-PVA nanocomposites

vibration of the OH^- group. The broad band centered near 3500 cm^{-1} has been assigned to sites that interact with residual physisorbed water [20]. The band at 1650 cm^{-1} observed in all spectra are attributed to stretching mode of hydroxyl group [21]. The spectrum of TiO_2-SiO_2 shows peaks at 1400 cm^{-1} and 550 to 450 cm^{-1} exhibiting stretching modes of Ti-O-Ti. The peak at 1100 cm^{-1} shows Si-O-Si bending vibrations and the peak at 1005 cm^{-1} shows Si-O-Ti vibration modes which are due to the overlapping from vibrations of Si-OH and Si-O-Ti bonds. These results indicate that TiO_2-SiO_2 nanoparticles were prepared by a combination of TiO_2 with SiO_2 [21]. SEM-EDS spectra shows the presence of metal oxide bonds in both samples (Table-2).

TABLE-2
EDS RESULT FOR TiO_2-SiO_2-20 AND TiO_2-SiO_2-30

Element	TiO_2-SiO_2-20		TiO_2-SiO_2-30	
	Mass (%)	Mole (%)	Mass (%)	Mole (%)
SiO_2	10.57	7.82	13.88	10.20
TiO_2	67.41	77.22	69.63	79.61
C	22.02	14.95	16.49	10.18
Total	100	100	100	100

Fig. 3 shows the SEM-EDS images along with particle size distribution of the colloidal TiO_2-SiO_2 nanocomposites. The TiO_2-SiO_2 particles exhibited irregular morphology due to the agglomeration of primary particles. But the colloidal TiO_2-SiO_2 nanocomposites exhibited regular morphology since the TiO_2-SiO_2 were coated by polyvinyl alcohol, which was confirmed by transmission electron microscopy image (Fig. 4). These results indicate that TiO_2-SiO_2 nanoparticles were prepared by a combination of TiO_2 with SiO_2 nanoparticles [2,22]. SEM-EDS results show the presence of metal oxide bonds in both samples.

Fig. 4 shows the TEM of TiO_2-SiO_2-20 and TiO_2-SiO_2-30 composites calcined at 500 °C. TiO_2-SiO_2 composite calcined at the same temperature has an average particle size (DTEM) smaller than 20 nm. From this observation, it is confirmed that the addition of silica is inhibiting the crystal growth of titania by providing a barrier between titania grains [17].

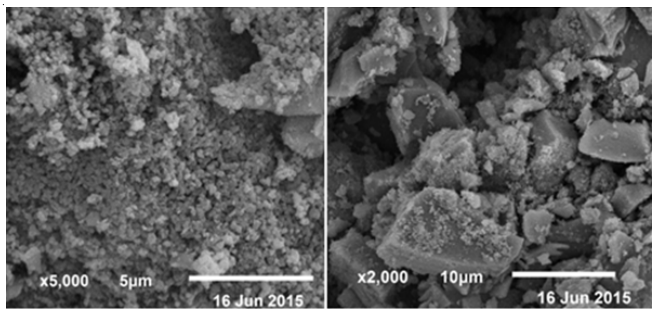

Fig. 3. SEM images for nanosized TiO_2-SiO_2

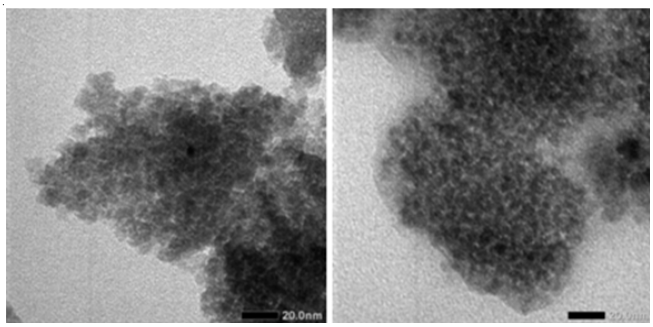

Fig. 4. TEM images of composites, (a). TiO_2-SiO_2-20 and (b). TiO_2-SiO_2-30

Effect of the ratio of TiO_2-SiO_2 on the degradation of Methylene blue: The photocatalytic oxidation of as-prepared pure TiO_2 and nanocomposite TiO_2-SiO_2 are shown in Fig. 5. The figure shows a decrease of absorbance of methylene blue by nanoparticle TiO_2 and TiO_2-SiO_2 nanocomposites. The absorbance of methylene blue decreased exponentially with irradiation time. The highest percentage of degradation of methylene blue is indicated by TiO_2-SiO_2-30 nanocomposite. The photocatalytic activity of TiO_2 is lower than all synthesized TiO_2-SiO_2 nanocomposites. Decomposition of methylene blue showed that the degradation percentage depends on the mole ratio of TiO_2/SiO_2. Composite TiO_2-SiO_2-30 provides the highest percent degradation. This likely is due to the increase in the surface area of the composite and the increasing homogeneity of the particles under the influence of polyvinyl alcohol during synthesis. This is also shown by the results of the measurement of surface area by BET method. The increase in reactivity can partly be attributed to an increased homogeneity of the nanocomposites and also the beneficial effect of SiO_2, which indicates no photo activity, but is probably related to the preferential adsorption of methylene blue. The preferential adsorption effectively increases the surface concentration of methylene blue at or near the TiO_2 sites promoting more efficient oxidation by photogenerated species [23].

Antibacterial activity of TiO_2-SiO_2 composites: The synthesized TiO_2 and TiO_2-SiO_2 nanocomposites were evaluated for antimicrobial activity (Fig. 6). The method for testing an antibacterial activity is the agar dilution method to determine the inhibitory concentration of antimicrobial agents [24] against *E. coli*. The Gram-negative bacteria have only a thin layer of peptidoglycan and a more complex cell wall with two cell membranes, an outer membrane and a plasma membrane. Under certain conditions, the Gram-negative bacteria are more resistant to many chemical agents than the Gram-positive cells [25].

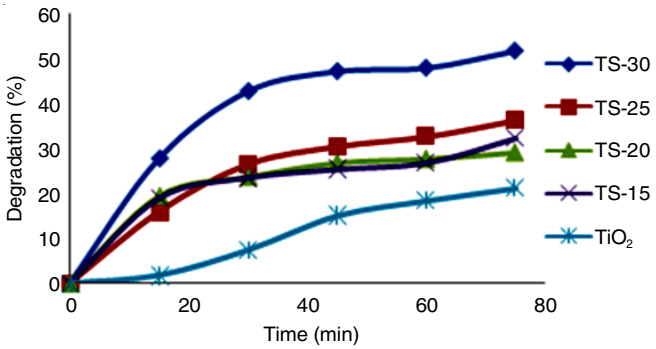

Fig. 5. Decomposition of methylene blue solution with various TiO_2-SiO_2 nanoparticle

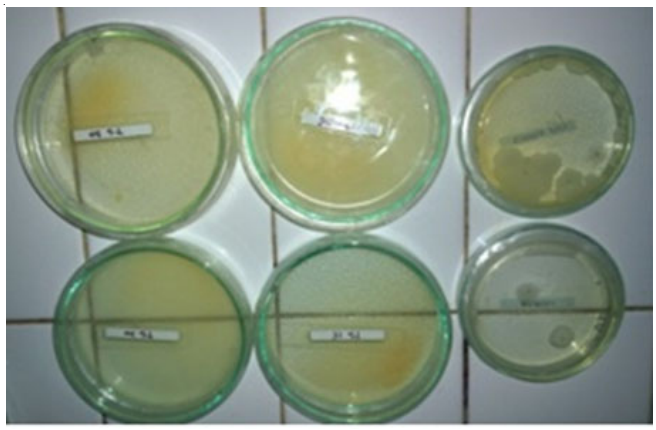

Fig. 6. Antimicrobial testing by agar dilution method

The results of antimicrobial testing were listed in Table-3. The concentration of the composite for antimicrobial testing was 50 mg/mL. The results showed that the bacterial inactivation was strongly enhanced in the presence of photo-activated anatase TiO_2 nanoparticles. While in the absence of photo-activated nanoparticles, no inhibition was observed. Hence, times of exposure to UV light, the amount of TiO_2 or TiO_2-SiO_2 and duration of exposure are factors found to be responsible for taken for 100 % killing of the bacterial population. The study indicates that the low concentration of TiO_2 is sufficient to control the diversity of the bacterial population.

TABLE-3
ACTIVITY OF SYNTHESIZED MATERIALS IN AGAR MEDIUM

Sample name	Treatment	Growth of bacteria
TiO_2	UV 368 nm	No growth
TiO_2-SiO_2-15	UV 368 nm	No growth
TiO_2-SiO_2-20	UV 368 nm	No growth
TiO_2-SiO_2-25	UV 368 nm	No growth
TiO_2-SiO_2-30	UV 368 nm	No growth
TiO_2-SiO_2-25	No UV	Growth
TiO_2-SiO_2-30	No UV	Growth
Blank	UV 368 nm	Growth

Conclusion

The nanosized TiO_2 mixed with SiO_2 sphere was prepared by sol-gel process. The major phase of the pure TiO_2 particle and deposited TiO_2 on SiO_2 sphere are of the anatase structure. In photodecomposition, a batch reactor was used to study the degradation of methylene blue by TiO_2-SiO_2 and pure TiO_2 particles. A mixed oxide TiO_2-SiO_2 is a more efficient photo-catalyst for the degradation of methylene blue than TiO_2 alone. In this study, the composite material was tested the antibacterial activity for *E. coli* bacteria. All the four synthesized samples showed inactivation activity towards bacteria by illuminating with UV 368 nm.

ACKNOWLEDGEMENTS

The authors are thankful to Laboratory of Microbiology, Department of Biology, Universitas Negeri Semarang and Department of Chemistry, Universitas Negeri Semarang, for providing all research facilities to complete this work. The authors are also grateful to Directorate General of Higher Education, for providing financial support.

REFERENCES

1. Y. Chen, K. Wang and L. Lou, *J. Photochem. Photobiol. Chem.*, **163**, 281 (2004).
2. K. Balachandaran, R. Venckatesh and R. Sivaraj, *Int. J. Eng. Sci. Res. Technol.*, **2**, 3695 (2010).
3. E. Rahmani, A. Ahmadpour and M. Zebarjad, *Chem. Eng. J.*, **174**, 709 (2011).
4. M. Anpo, *J. Catal.*, **216**, 505 (2003).
5. R. Zhang, L. Gao and Q. Zhang, *Chemosphere*, **54**, 405 (2004).
6. P.S. Awati, S.V. Awate, P.P. Shah and V. Ramaswamy, *Catal. Commun.*, **4**, 393 (2003).
7. A. Mirabedini, S.M. Mirabedini, A.A. Babalou and S. Pazokifard, *Prog. Org. Coat.*, **72**, 453 (2011).
8. G. Fu, P.S. Vary and C.T. Lin, *J. Phys. Chem. B*, **109**, 8889 (2005).
9. H. Nur, *Mater. Sci. Eng. B*, **133**, 49 (2006).
10. L. Song, R. Qiu, Y. Mo, D. Zhang, H. Wei and Y. Xiong, *Catal. Commun.*, **8**, 429 (2007).
11. X. Gao and I.E. Wachs, *Catal. Today*, **51**, 233 (1999).
12. A. Matsuda, T. Matoda, Y. Kotani, T. Kogure, M. Tatsumisago and T. Minami, *J. Sol-Gel Sci. Technol.*, **26**, 517 (2003).
13. S.I. Seok and J.H. Kim, *Mater. Chem. Phys.*, **86**, 176 (2004).
14. R. Venckatesh, K. Balachandaran and R. Sivaraj, *Int. Nano Lett.*, **2**, 15 (2012).
15. S. Bonetta, S. Bonetta, F. Motta, A. Strini and E. Carraro, *AMB Express*, **3**, 59 (2013).
16. U. Sirimahachai, S. Phongpaichit and S. Wongnawa, *Songklanakarin J. Sci. Technol.*, **31**, 517 (2009).
17. C. Randorn, S. Wongnawa and P. Boonsin, *Sci. Asia*, **30**, 149 (2004).
18. J. Gao, S. Li, W. Yang, G. Zhao, L. Bo and L. Song, *Rare Metals*, **26**, 1 (2007).
19. K.V. Baiju, P. Periyat, P.K. Pillai, P. Mukundan, K.G.K. Warrier and W. Wunderlich, *Mater. Lett.*, **61**, 1751 (2007).
20. U. Sirimahachai, N. Ndiege, R. Chandrasekharan, S. Wongnawa and M.A. Shannon, *J. Sol-Gel Sci. Technol.*, **56**, 53 (2010).
21. J. Rubio, J.L. Oteo, M. Villegas and P. Duran, *J. Mater. Sci.*, **32**, 643 (1997).
22. M. Zhang, L. Shi, S. Yuan, Y. Zhao and J. Fang, *J. Colloid Interface Sci.*, **330**, 113 (2009).
23. C. Anderson and A.J. Bard, *J. Phys. Chem.*, **99**, 9882 (1995).
24. V.S. Smitha, K.A. Manjumol, K.V. Baiju, S. Ghosh, P. Perumal and K.G.K. Warrier, *J. Sol-Gel Sci. Technol.*, **54**, 203 (2010).
25. G. Tortora, R.B. Funke and L.C. Case, Microbiology: An Introduction, Addison-Wesley Longman, Inc., New York, USA (2001).